AD-A124 140 EFFECTS OF SHORT GLASS FIBERS AND PARTICULATE FILLERS 1/1
ON FATIGUE CRACK PROPAGATION IN POLYAMIDES(U) LEHIGH
UNIV BETHLEHEM PA COXE LAB R W LANG ET AL. DEC 82
UNCLASSIFIED TR-12 N00014-77-C-0633 F/G 11/2 . NL

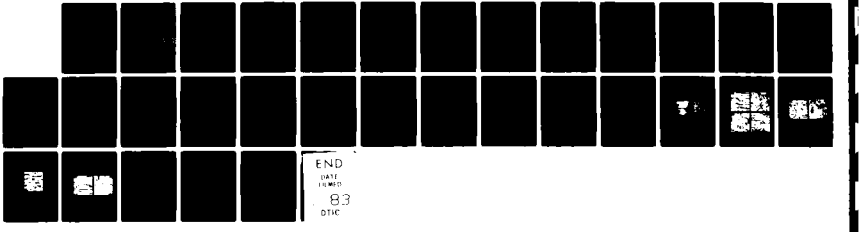

END
DATE FILMED
83
DTIC

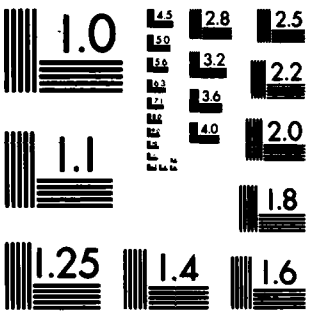

SECURITY CLASSIFICATION OF THIS PAGE (When Data Entered)

REPORT DOCUMENTATION PAGE

READ INSTRUCTIONS BEFORE COMPLETING FORM

1. REPORT NUMBER: Technical Report #12	2. GOVT ACCESSION NO.: AD A124140
3. RECIPIENT'S CATALOG NUMBER	
4. TITLE (and Subtitle): Effects of Short Glass Fibers and Particulate Fillers on Fatigue Crack Propagation in Polyamides	5. TYPE OF REPORT & PERIOD COVERED: Technical Report
	6. PERFORMING ORG. REPORT NUMBER
7. AUTHOR(s): R. W. Lang, J. A. Manson, and R. W. Hertzberg	8. CONTRACT OR GRANT NUMBER(s): N00014-77-C-0633
9. PERFORMING ORGANIZATION NAME AND ADDRESS: Materials Research Center, Lehigh University, Bethlehem, PA 18015	10. PROGRAM ELEMENT, PROJECT, TASK AREA & WORK UNIT NUMBERS: NR356-670
11. CONTROLLING OFFICE NAME AND ADDRESS: Office of Naval Research, 800 N. Quincy Street, Arlington, VA 22217	12. REPORT DATE: December 1981
	13. NUMBER OF PAGES
14. MONITORING AGENCY NAME & ADDRESS(if different from Controlling Office)	15. SECURITY CLASS. (of this report): Unclassified
	15a. DECLASSIFICATION/DOWNGRADING SCHEDULE

16. DISTRIBUTION STATEMENT (of this Report)

This document has been approved for public release; its distribution is unlimited.

17. DISTRIBUTION STATEMENT (of the abstract entered in Block 20, if different from Report)

DTIC ELECTE FEB 7 1983 S D A

18. SUPPLEMENTARY NOTES

Prepared for publication in Polymer Engineering and Science

19. KEY WORDS (Continue on reverse side if necessary and identify by block number)

Polyamides	Particulate-reinforced plastics
Nylon 6	Fracture
Nylon 66	Fracture mechanisms
Fiber-reinforced plastics	Fatigue

20. ABSTRACT (Continue on reverse side if necessary and identify by block number)

The fatigue crack propagation (FCP) behavior (at 10 Hz) of several commercial short-glass-fiber and mineral-reinforced nylon composites has been investigated. The FCP rates can be described in terms of the well known Paris relationship. Significant improvement in FCP performance was found for the glass-fiber-reinforced materials in comparison to that of the pure matrix materials (nylon 66 and nylon 612). Also, the FCP resistance was found to increase with increasing fiber content and interfacial adhesion for nylon 66. Despite

DD FORM 1 JAN 73 1473 EDITION OF 1 NOV 65 IS OBSOLETE S/N 0102-014-6601

SECURITY CLASSIFICATION OF THIS PAGE (When Data Entered)

the fact that specimens were cut from injection-molded plaques, no or only slight effects of orientation were observed by testing specimens with cracks growing parallel and perpendicular, respectively, to the major flow direction. Electron microscopy studies of fracture surfaces revealed a complex pattern of fiber orientation varying over the plaque thickness and consisting of layers with fibers oriented mainly parallel, perpendicular or randomly to the major flow direction; nevertheless, the specimens behaved quasi-isotropically. Significant differences in fracture mechanism were observed depending on the matrix, the interfacial bonding, and the crack speed. In contrast to the fiber-reinforced nylons, the mineral-reinforced material exhibited poorer FCP resistance than neat nylon 66, even though the former is superior in tensile and impact behavior.

OFFICE OF NAVAL RESEARCH

Contract N00014-77-C-1234

Task No. NR 056-123

TECHNICAL REPORT NO. 12

Effects of Short Glass Fibers and Particulate Fillers on Fatigue Crack Propagation in Polyamides

by

Reinhold W. Lang, John A. Manson and Richard W. Hertzberg

Prepared for Publication

in

Polymer Engineering and Science

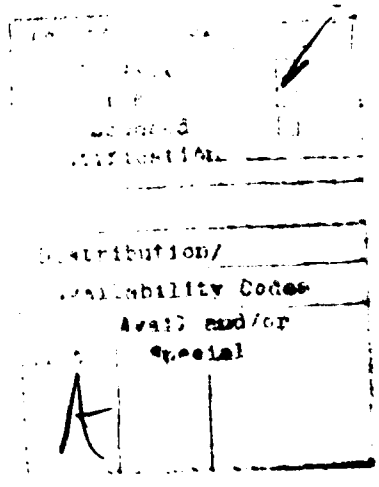

Materials Research Center
Coxe Laboratory 32
Lehigh University
Bethlehem, Pennsylvania 18015

December 1982

Effect of Short Glass Fibers and Particulate Fillers on Fatigue Crack Propagation in Polyamides

R. W. Lang, J. A. Manson, and R. W. Hertzberg
Lehigh University
Materials Research Center
Bethlehem, PA 18015

Abstract

The fatigue crack propagation (FCP) behavior (at 10 Hz) of several commercial short-glass-fiber and mineral-reinforced nylon composites has been investigated. The FCP rates can be described in terms of the well known Paris relationship. Significant improvement in FCP performance was found for the glass-fiber-reinforced materials in comparison to that of the pure matrix materials (nylon 66 and nylon 612). Also, the FCP resistance was found to increase with increasing fiber content and interfacial adhesion for nylon 66. Despite the fact that specimens were cut from injection-molded plaques, no or only slight effects of orientation were observed by testing specimens with cracks growing parallel and perpendicular, respectively, to the major flow direction. Electron microscopy studies of fracture surfaces revealed a complex pattern of fiber orientation varying over the plaque thickness and consisting of layers with fibers oriented mainly parallel, perpendicular or randomly to the major flow direction; nevertheless, the specimens behaved quasi-isotropically Significant differences in fracture mechanism were observed, depending on the matrix, the interfacial bonding, and the crack speed. In contrast to the fiber-reinforced nylons, the mineral-reinforced material exhibited poorer FCP resistance than neat nylon 66, even though the former is superior in tensile and impact behavior.

Introduction

Since rigid inorganic phases (both fibrous and particulate) are often combined with plastics to yield composites for engineering applications, their fatigue behavior is of considerable interest. For example, the S-N or E-N behavior (cyclic stress or modulus vs. cyclic life) of many fibrous composites has been extensively investigated. Failure processes have also been studied, often using fracture mechanics approaches, and much of the cyclic life is often associated with the propagation of damage from a flaw (1). [For reviews, see references 2-5.] Indeed several studies of FCP in short-fiber and particle-reinforced composites have been reported (6-9). However, while some S-N curves compare the matrix with the composite (10), most of the available FCP data do not permit ready comparison. [For an exception, see Suzuki et al. (11), who showed that short glass fibers decreased FCP rates in nylon 6.]

We decided therefore to extend our current studies of FCP in engineering plastics [e.g., polyamides (12,13)] to include particle and short-fiber reinforced systems. The goal is to examine FCP response and the micromechanisms of failure as a function of test conditions, composition, orientation, interfacial characteristics (14), and environment. This paper describes preliminary results with several readily available composites of nylon 66 (N66) and nylon 612 (N612); later papers will describe results for made-to-order systems including specific interfacial treatments.

Experimental

Materials and Specimen Preparation

Table 1 lists the materials tested and their sources and characteristics. All plaques were injection-molded, with dimensions and gating

indicated in Fig. 1. Since injection-molding yields complex orientations of fibers, specimens were cut to be loaded transversely (T) or longitudinally (L) with respect to the flow direction. Values of the number average molecular weight, M_n, were determined viscometrically in formic acid (15); % crystallinity was determined using a density gradient column; values of E were of flexural modulus (16,17), except for series B, in which the storage modulus, E', was measured using an Autovibron, model IIIC (Imass, Hingham, Mass.).

To examine the role of notch sharpness on the fracture energies of A-N66 and A-40M, respectively, impact tests were performed on specially prepared specimens. Two sets of samples of identical geometry containing either a machined notch or a fatigue crack were used for each of these materials. In the one case a notch 5.1 mm in length was cut with a single-point cutter having a tip radius of approximately 0.5 mm. In the other case a notch only 2.5 mm long was machined and the specimens were subsequently fatigued at 10 Hz in a 4-point bending apparatus to grow a fatigue crack of 2.6 mm. Thus the total length of the crack (i.e., of the machined notch plus the fatigue crack) was also 5.1 mm. The specific fracture energy, W_{sp}, (fracture energy W/cross-sectional area of unbroken ligament A), was determined using an Izod impact tester, TMI No. 43-1 (Testing Machines, Inc., Amityville, New York).

Fatigue Testing

Tests were conducted using an electrohydraulic closed loop testing machine at a frequency of 10 Hz using standard procedures and compact-tension specimens (18). The applied waveform was sinusoidal with constant load amplitude and a minimum-to-maximum load ratio, R, of 0.1. Environmental conditions were laboratory air at 22-24°C and a 40% average relative

humidity. FCP rates were plotted as log da/dN, the rate of crack growth per cycle, as a function of log ΔK, the stress-intensity-factor range; ΔK is given by $\Delta K = Y\Delta\sigma\sqrt{a}$, where Y is a geometrical variable, $\Delta\sigma$ the stress range and a the crack length. After coating with a 15-to-20-nm-thick gold-palladium layer, fracture surface morphologies were studied with an ETEC scanning electron microscope (SEM) (20-kV accelerating voltage).

Results and Discussion

Fatigue Crack Propagation

The effects of different second phases on FCP resistance in a dry nylon matrix are evident in the comparison with pure N66 in Fig. 2; the figure also shows that macroscopic growth rates were essentially the same for samples tested in longitudinal (L) and transverse (T) directions. This is reasonable for the particle-reinforced material; for discussion of the independence of FCP rate on orientation in the fiber-reinforced nylons, see the section Fractography. In any case, while the FCP resistance is decreased by the particulate filler in A-40M, a significant improvement can be observed for the short-glass-fiber reinforced material. In fact, on extrapolating the curves to $\Delta K = 2.5$ MPa$\sqrt{m}$, FCP rates increase by about 1.5 orders of magnitude for A-40M, but decrease by more than 2 orders of magnitude for A-33G. An alternative comparison is based on the ΔK necessary to drive the crack at a given rate. The ΔK required for $da/dN = 10^{-3}$ mm/cycle, for instance, is 2, 3, and $\sim$6 MPa$\sqrt{m}$ for A-40M, A-N66, and A-33G, respectively. Thus the substantial improvement in other mechanical properties (10,16,17, Table 1) due to the incorporation of short glass fibers is also reflected in FCP behavior.

On the other hand, the detrimental effect on FCP performance due to the presence of the mineral filler (A-40M) seemed at first to be somewhat surprising. Although the matrix in A-40M has not been identified, values of notched impact strength, tensile strength, and especially modulus, E, are all higher than for N66 (16,17); also, fatigue cracks were more difficult to initiate in A-40M than N66. Hence it appears that A-40M is more sensitive to notch acuity and requires more energy to initiate a crack than N66. Since conventional tensile tests or impact tests do not distinguish between the energy dissipated in initiation and the energy dissipated in propagation of fracture, it was decided to separate these two parts by testing the impact properties of specimens containing a machined notch (notch tip radius, ≈0.5 mm) versus specimens having a fatigue crack of the same length. It is apparent from the results shown in Table 2 that the specific fracture energy is higher for A-40M than for A-N66 in the case of the machine notched samples. Also, W_{sp} in the pure nylon 66 is slightly higher for the fatigue-cracked sample (by a factor of 1.3), probably due to blunting by the cyclically-induced plastic zone at the crack tip. On the other hand, the specific fracture energy for A-40M is reduced by more than an order of magnitude when a fatigue crack replaces a machined notch. As a consequence the relative ranking of the two materials becomes inverted in this case, paralleling the results obtained for FCP. These observations clearly confirm the assumption of the higher energy necessary to initiate a crack in A-40M. However, once a sharp crack is present it propagates more readily in the particle-reinforced material.

The effect of fiber concentration (0, 30, and 50 wt %) is shown for the case of series B (based on nylon 66) in Fig. 3. While the values shown

are for the T-configuration, results for the L-configuration were similar. Clearly, as found for fatigue life in unnotched specimens (10) and for FCP in nylon 6 (11), the FCP resistance increases with fiber content, at least at a frequency of 10 Hz. [For a study of the effects of frequency in these composites, see reference 19.] However, several differences between the data in Figs. 2 and 3 are apparent. First, B-N66 behaves better than A-N66, the difference in da/dN being nearly an order of magnitude. Although the water content differs (Table 1), the average molecular weight and crystallinity are similar. While water has a profound effect on FCP in nylons, comparison of these data with those from references 12 and 13 shows that water alone cannot account for the difference mentioned. It seems likely that specimen thickness (6 and 3 mm for A-N66 and B-N66, respectively) is at least partly responsible. The thinner the specimen, the greater the tendency towards plane-stress rather than plane-strain conditions, and the greater the energy required to propagate the crack. Indeed, as with polycarbonate (20,21), shear lips were observed on the fracture surfaces of B-N66 (19). Second, while FCP resistance in series B is increased with increasing fiber content, a comparison of Series A and B (Figs. 2 and 3) shows that the FCP resistance of A-33G is superior to that of both B-30G and B-50G. This may be due to differences in fiber aspect ratios and interfacial bond strengths. In fact, SEM studies of fracture surfaces (see below) reveal a greater degree of fiber-matrix adhesion for materials of series A; thus series A would be expected to behave better than series B. In any case, both aspect ratio and interfacial adhesion are known to be important factors in fatigue life and other kinds of mechanical response as well (2-9,22).

Preliminary tests (Fig. 4) were also conducted using N612 reinforced with 43% glass fibers (C-43G), and compared with those for the pure matrix

(12,13). The improvement by the incorporation of fibers is again remarkable. [It should be noted that for both C-N612 (12) and C-43G some dependence on orientation was observed.]

Fractography

Fig. 5 shows two failed specimens of A-33G arranged as cut from the original plaque (Fig. 1); as can be seen, the cracks propagated nominally parallel to the anticipated crack plane. [For some specimens (N66 with 43% fibers), the test results had to be discarded because of excessive departure of the crack from the desired horizontal fracture plane due to fiber orientation.]

Fractographic examinations were conducted to determine the orientation of fibers in the fibrous systems, and to provide insight into the mechanisms of FCP. It was discovered that the fiber orientation varied over the thickness of the injection-molded plaques as if they were composed of several different layers. The following model might be useful to describe these findings. Close to the two surfaces of the plaques where the shear gradient (or velocity gradient) in the melt stream while filling the mold is high, fibers are oriented mainly parallel to the major flow direction (that is, the L-direction in Fig. 1). On the other hand, in the central or core region the fiber orientation is perpendicular to the flow direction. This is due to the domination of a strain flow effect caused by the expansion of the melt stream in the T-direction after passing through the narrow gate into the much wider mold. Between the center and surface layers there are intermediate layers where neither shear-gradient nor strain-flow effects are prevalent, leading to a more or less random orientation of fibers in the L-T plane.

The investigation of the various fracture surfaces revealed that this simplified model can reasonably describe and interpret the fiber orientation in the materials studied, at least qualitatively. This also may explain why most of the materials exhibited behavior that was independent of orientation; they behaved quasi-isotropically. It was difficult to quantitatively measure the thicknesses of layers with different orientations since the determination of boundaries between oriented and random layers can only be done arbitrarily. However, C-43G, in which some orientation effects in FCP were observed (see Fig. 4), did also exhibit clear differences in the thickness of the oriented layers.

Representative fractographs illustrating the effects discussed above are shown in Fig. 6 for A-33G. As can be seen, in changing the direction of load from T (Figs 6a and 6b) to L (Figs. 6c and 6d), the orientation of fibers on the fracture surface appears in an inverse order. For example fibers are oriented parallel in the surface layer (Fig. 6a) and in the core layer (Fig. 6d) of the fracture surfaces of A-33G/T and A-33G/L respectively. The same pattern holds for fibers oriented normal to the fracture surface. Similar observations with regard to fiber orientation in injection-molded discs of glass-fiber-reinforced thermoplastics have also been reported by Darlington and others (24).

The fractographs depicted in Fig. 6 for A-33G also reveal some interesting features with respect to the fracture mechanism in the region of stable crack growth. When fibers are oriented parallel to the fracture surface appreciable drawing of the nylon 66 matrix is visible, indicative of ductile failure. On the contrary, in regions where fibers are normal to the fracture surface, matrix fracture appears to be rather brittle in nature;

failure occurs by fiber breakage rather than by fiber pull-out. The nylon 612-based composites behaved in a similar fashion (see Fig. 7).

In contrast, the fracture surface appearance was quite different in the fast fracture region. In general, matrix fracture was more brittle in the dry composites of N66 and N612 (Series A and C) independent of fiber orientation. Furthermore, contrary to the observations in the stable crack growth region, considerable fiber pull-out was typical in areas where fibers were oriented normal to the fracture surface. An example is shown in Fig. 8 for C-43G. It should be mentioned that these results resemble the findings by Mandell, et al. (25,26) who reported that the local mode of crack extension in glass-reinforced materials is predominantly one of fiber-avoidance but that fiber failure can be observed when a crack is intentionally grown from a notch (slow growth rate). Most strikingly, however, while fibers on the fracture surface appeared to be smooth and mirror-like when the crack propagated in a stable fashion (Figs. 6 and 7), a high degree of interfacial adhesion was revealed by materials of Series A and C where fast fracture occurred (Figs. 8 and 9a). At present the cause of the difference in interfacial failure is not known; interestingly, Mandell et al. (25) did not observe such differences in their fracture surfaces.

Finally, the effect of fiber-matrix adhesion on FCP is also of interest (see discussion of Series A and B above). Whereas differences in interfacial strength between the nylon-66 based composites of Series A and B were not clearly evident in the region of slow crack growth, fracture surfaces did appear quite different in the fast fracture region (Fig. 9). Thus, it can be seen that the interfacial strength is lower in the composites of Series B where 1.7% water is present (clean and mirror-like fibers in Fig. 9b). Also the matrix for these materials reveals a much higher degree

of ductility due to both plasticization and the higher temperature increase during cyclic loading as a result of increased hysteretic energy losses associated with the presence of imbibed water (27). [For crack tip temperature data of Series B see (19)]. While it is not yet known whether the interfacial weakness is due to attack by water or to a less effective surface treatment of the fibers in the latter case, the effect on FCP is deleterious. Thus the beneficial effect of small amounts of water on the FCP response found in unreinforced nylon 66 (13) may be overbalanced by the creation of a weak interface in the composites.

Conclusions

Clearly more research needs to be done on elucidating in detail the effects of specimen thickness, fiber length and aspect ratio (after processing), interfacial bonding, orientation, and environment. So far, however, several observations and conclusions may be noted:

1. The resistance of typical nylon to fatigue crack propagation can be significantly increased by the incorporation of short glass fibers.

2. The increase in FCP resistance increases with increasing fiber content, presumably reflecting an increase in both modulus and fracture energy.

3. Clear differences are seen in the fracture surfaces obtained during stable and unstable crack growth, reflecting variations in the balance between fiber fracture and fiber pull-out. Variations in the extent of interfacial separation were also seen, possibly depending on the fiber surface treatment or the water content.

4. In contrast, a particulate mineral-reinforced composite exhibited lower resistance to fatigue crack propagation than neat nylon 66, even though

the former has a higher modulus and tensile and notched impact strengths. While this composite required a higher energy to initiate fracture than nylon 66, a crack, after being initiated propagated more readily.

References

1. M. J. Owen, T. R. Smith and R. Dukes, Plast. Polym. 37 227 (1969).

2. L. J. Broutman and R. H. Krock (eds.), "Composite Materials," 8 vols. Academic Press, New York, (1974).

3. J. A. Manson and L. H. Sperling, "Polymer Blends and Composites," Plenum Press, New York, (1976).

4. B. D. Agarwal and L. J. Broutman, "Analysis and Performance of Fiber Composites," Wiley, New York, (1980).

5. R. W. Hertzberg and J. A. Manson, "Fatigue in Engineering Plastics," Academic, New York, (1980).

6. P. A. Thornton, J. Composite Mater. 6, 147 (1972).

7. M. J. Owen and P. T. Bishop, J. Phys. D: Appl. Phys. 7, 1214 (1974).

8. A. T. DiBenedetto and G. Salee, Tech. Rep. AMMRC CTR 77-12 (March 1977).

9. J. Lankford, W. J. Astleford, and M. A. Asher, J. Mater. Sci. 11, 1624 (1976).

10. J. Theberge, B. Arkles, and R. Robinson, Ind. Eng. Chem. Prod. Res. Dev. 15 100 (1976).

11. M. Suzuki, M. Shimizu, E. Jinen, M. Maeda, and M. Nakamura, Proc. Int. Conf. on Mech. Behavior of Materials, Vol. 5, Kyoto, 279 (August 15, 1971).

12. P. E. Bretz, R. W. Hertzberg and J. A. Manson, J. Mater. Sci., 14, 2482 (1979).

13. P. E. Bretz, R. W. Hertzberg, and J. A. Manson, J. Mater. Sci., 16, 2061 (1981).

14. J. Williams and J. A. Manson, Org. Coatings Plast. Chem., 41(1), 175 (1980).

15. M. I. Kohan, "Nylon Plastics," Wiley, New York, 107 (1973).

16. E. I. duPont de Nemours & Co., n. d.

17. B. N. Epstein, Proc. S.P.I. Ann. Tech. Conf., 34th, Section 10-A (1979).

18. S. L. Kim, M. D. Skibo, J. A. Manson, and R. W. Hertzberg, Polym. Eng. Sci. 17, 194 (1977).

19. R. W. Lang, J. A. Manson, and R. W. Hertzberg, Proceedings, US-Italy Symposium on Composite Materials, Capri, June, 1981, in press.

20. G. Pitman and I. Ward, J. Mater. Sci., 15, 635 (1980).

21. J. A. Manson and R. W. Hertzberg, Crit. Rev. Macromol. Sci., 1 433 (1973).

22. R. E. Lavengood and L. E. Gulbransen, Polym. Eng. Sci. 9, 365 (1969).

23. L. C. Cessna, J. A. Levens, and J. B. Thomson, Polym. Eng. Sci. 9, 339 (1969).

24. M. W. Darlington, P. L. McGinley and G. R. Smith, J. Mater. Sci., 11 877 (1980).

25. J. F. Mandell, D. D. Huang, and F. J. McGarry, Polym. Compos., 2, 137 (1981).

26. J. F. Mandell, Proc. 34th SPI Reinforced Plastics/Composites Institute, Section 20-C (1979).

27. M. T. Hahn, R. W. Hertzberg, J. A. Manson, R. W. Lang, and P. E. Bretz, submitted to Polymer, 1981.

Table 1. Materials, Specimen Designations and Sources

Material Designation[a]	Commercial Designation	Nylon Type	Reinforcement or Filler, wt.(vol)%	M_n x10^{-3}	% Cryst.	E, GPa
A-N66[b]	Zytel 101	66	—	18.5	39	2.83[d]
A-33G[b]	Zytel 70G 33	66	glass[e] fibers, 33 (18)	18.5	—	8.96[d]
A-40M[b]	Minlon 11C40	—	calcined clay, 40		—	5.30[d]
B-N66[c]	R-1000	66	—	19.0	42	2.50
B-30G[c]	RF-1006	66	glass[e] fibers, 30(16)	19.0	—	5.70
B-50G[c]	RF-10010	66	glass[e] fibers, 50(31)	19.0	—	7.30
C-N612[b]	Zytel 151	612	—	—	—	2.03[d]
C-43G[b]	Zytel 77G 43	612	glass[e] fibers, 43(24)	—	—	10.03[d]

[a] Series A and C (duPont) 6.4-mm thick; Series B (LNP) 3.2-mm thick. Geometry as in Fig. 1; symbols T and L added to the material designation refer to the direction of applied load.

[b] Dry, as-molded (~0.2% HOH).

[c] 1.7% HOH.

[d] Taken from the technical literature (16).

[e] E-glass

Table 2. Effects of machined and fatigued notches on specific fracture energy, W_{sp}, (on impact of A=N66 and A-40M.

Material	W_{sp}, kJ/m^2 (machined notch)	W_{sp}, kJ/m^2 (fatigued crack)	$\frac{W_{sp}\ (\text{fatigued})}{W_{sp}\ (\text{machined})}$
A-N66	2.30	2.96	1.3
A-40M	7.01	0.58	0.08

[a]Each value is the average of values for 4 specimens.

List of Figures

Lang, Fig. 1

SERIES A AND C

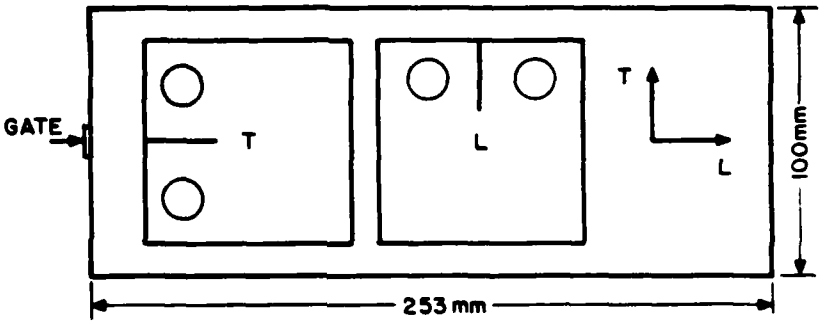

SERIES B

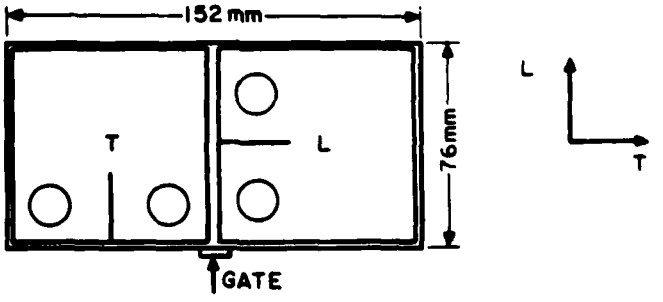

Lang, Fig. 2

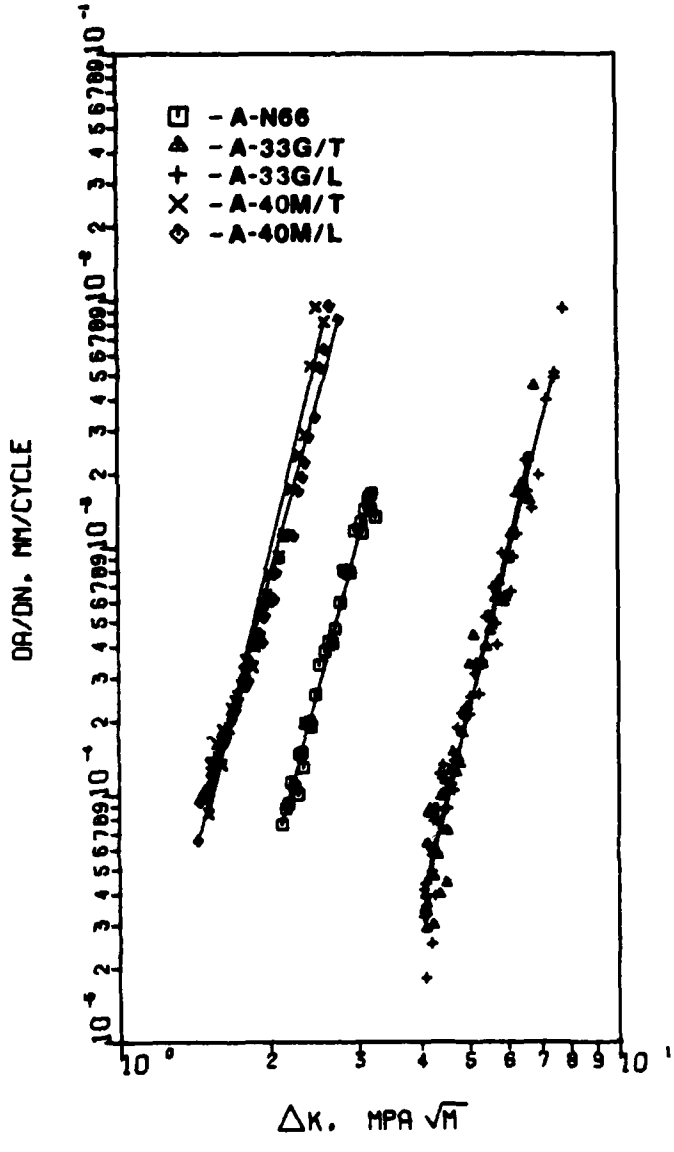

Lang, Fig. 3

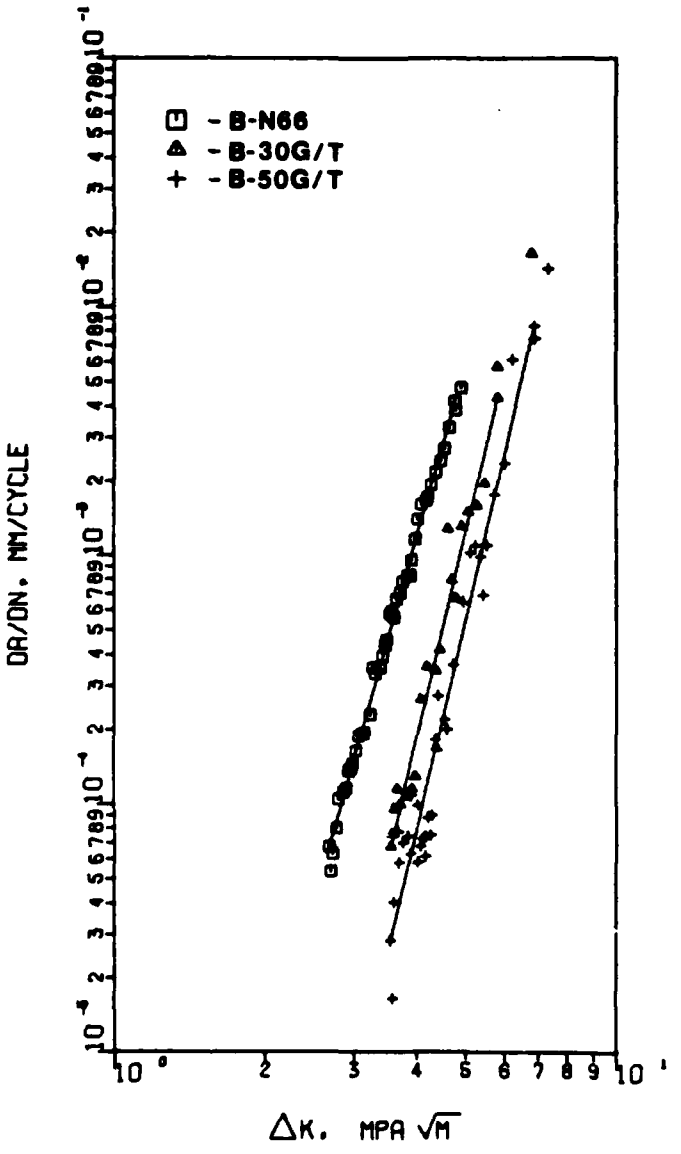

Lang, Fig. 4

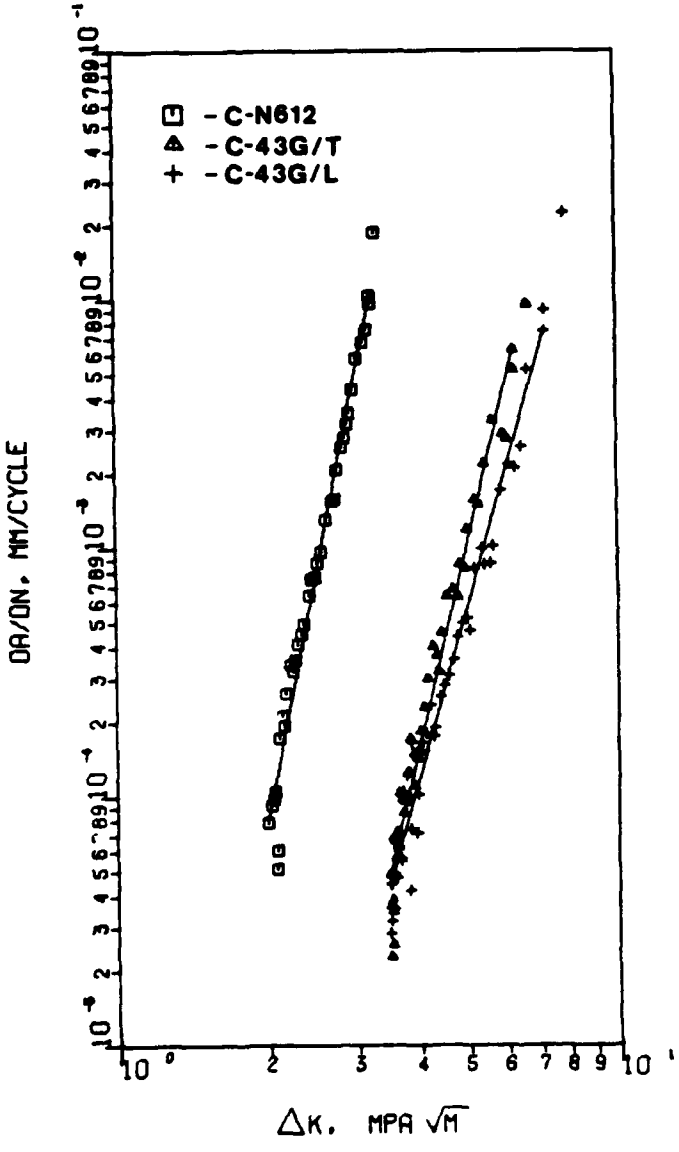

Lang, Fig. 5

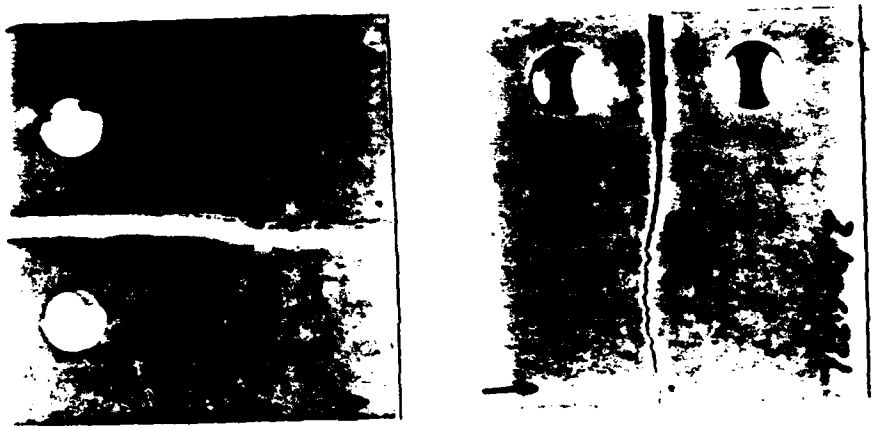

Lang, Fig. 6

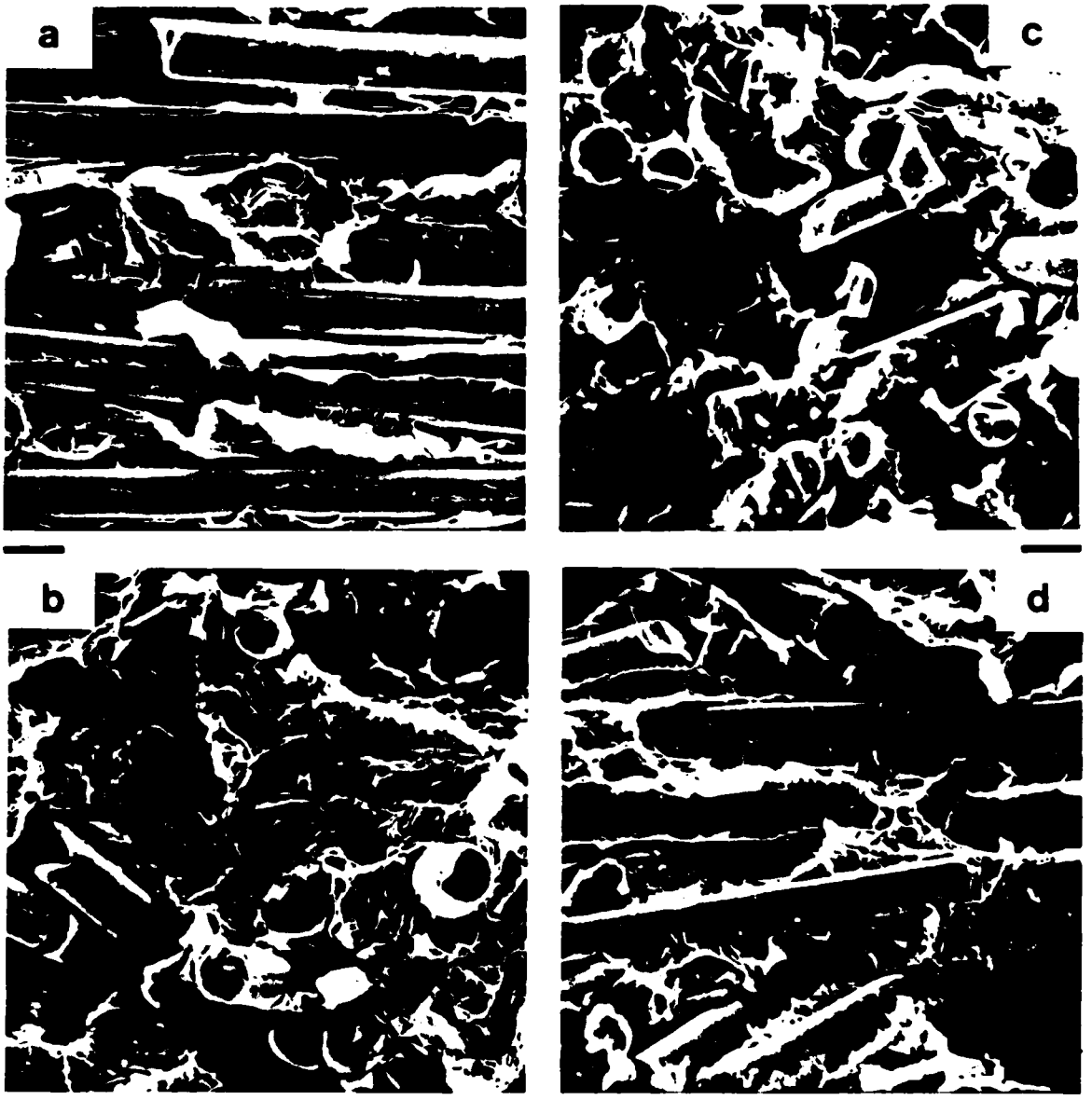

Lang, Fig. 7

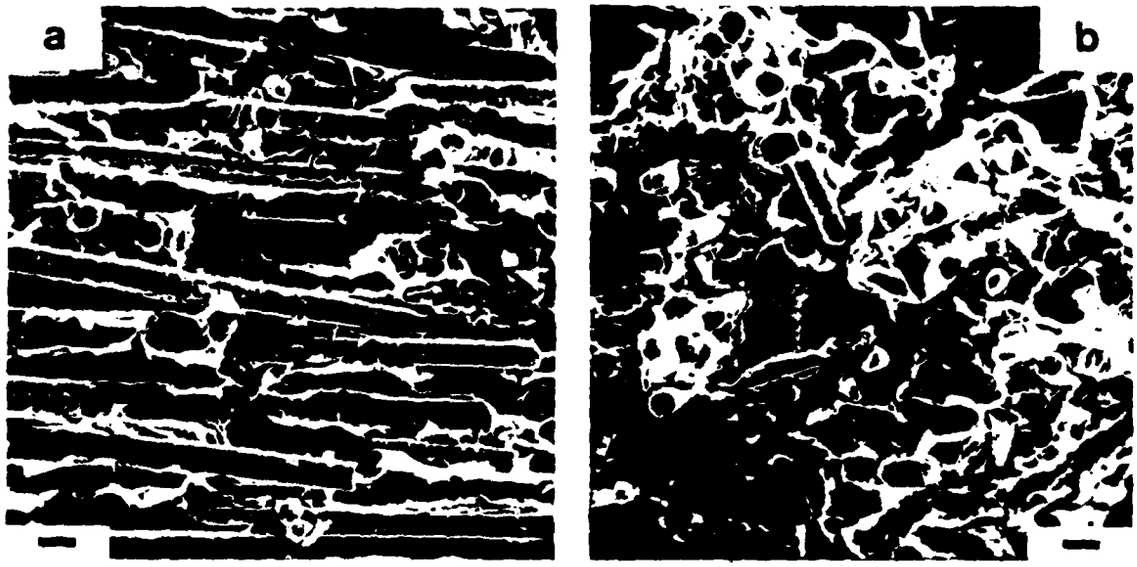

Lang, Fig. 8

Lang, Fig. 9

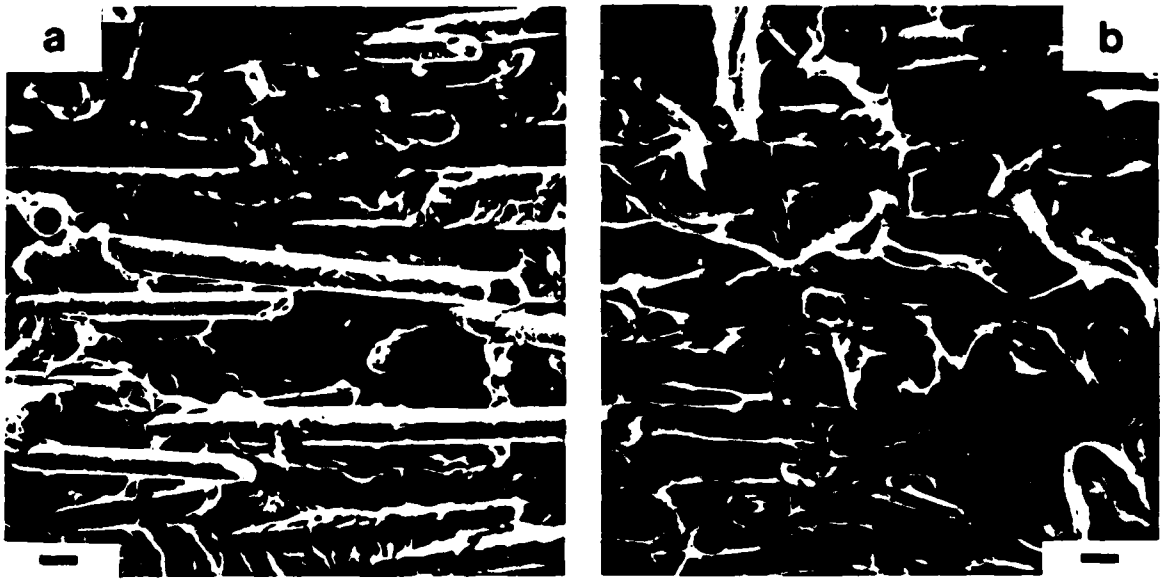

472:GAN:716-4
94/GEN

TECHNICAL REPORT DISTRIBUTION LIST, GEN

	No. Copies
Office of Naval Research Attn: Code 413 800 North Quincy Street Arlington, Virginia 22217	2
ONR Pasadena Detachment Attn: Dr. R. J. Marcus 1030 East Green Street Pasadena, California 91106	1
Commander, Naval Air Systems Command Attn: Code 310C (H. Rosenwasser) Department of the Navy Washington, D.C. 20360	1
Defense Technical Information Center Building 5, Cameron Station Alexandria, Virginia 22314	12
Dr. Fred Saalfeld Chemistry Division, Code 6100 Naval Research Laboratory Washington, D.C. 20375	1
U.S. Army Research Office Attn: CRD-AA-IP P. O. Box 12211 Research Triangle Park, N.C. 27709	1
Mr. Vincent Schaper DTNSRDC Code 2803 Annapolis, Maryland 21402	1
Naval Ocean Systems Center Attn: Dr. S. Yamamoto Marine Sciences Division San Diego, California 91232	1
Naval Ocean Systems Center Attn: Mr. Joe McCartney San Diego, California 92152	1
Naval Weapons Center Attn: Dr. A. B. Amster, Chemistry Division China Lake, California 93555	1
Naval Civil Engineering Laboratory Attn: Dr. R. W. Drisko Port Hueneme, California 93401	1
Dean William Tolles Naval Postgraduate School Monterey, California 93940	1
Scientific Advisor Commandant of the Marine Corps (Code RD-1) Washington, D.C. 20380	1
Naval Ship Research and Development Center Attn: Dr. G. Bosmajian, Applied Chemistry Division Annapolis, Maryland 21401	1
Mr. John Boyle Materials Branch Naval Ship Engineering Center Philadelphia, Pennsylvania 19112	1
Mr. A. M. Anzalone Administrative Librarian PLASTEC/ARRADCOM Bldg 3401 Dover, New Jersey 07801	1

9/82

TECHNICAL REPORT DISTRIBUTION LIST, 356A

	No. Copies
Dr. M. Broadhurst Bulk Properties Section National Bureau of Standards U. S. Department of Commerce Washington, D.C. 20234	2
Naval Surface Weapons Center Attn: Dr. J. M. Augl, Dr. B. Hartman White Oak Silver Spring, Maryland 20910	1
Dr. G. Goodman Globe Union Incorporated 5757 North Green Bay Avenue Milwaukee, Wisconsin 53201	1
Professor Hatsuo Ishida Department of Macromolecular Science Case-Western Reserve University Cleveland, Ohio 44106	1
Dr. David Soong Department of Chemical Engineering University of California Berkeley, California 94720	
Dr. Curtis W. Frank Department of Chemical Engineering Stanford University Stanford, California 94035	
Picatinny Arsenal Attn: A. M. Anzalone, Building 3401 SMUPA-FR-M-D Dover, New Jersey 07801	1
Dr. J. K. Gillham Department of Chemistry Princeton University Princeton, New Jersey 08540	1
Dr. E. Baer Department of Macromolecular Science Case Western Reserve University Cleveland, Ohio 44106	1
Dr. K. D. Pae Department of Mechanics and Materials Science Rutgers University New Brunswick, New Jersey 08903	1
NASA-Lewis Research Center Attn: Dr. T. T. Serofini, MS-49-1 2100 Brookpark Road Cleveland, Ohio 44135	1
Dr. Charles H. Sherman Code TD 121 Naval Underwater Systems Center New London, Connecticut 06320	1
Dr. William Risen Department of Chemistry Brown University Providence, Rhode Island 02191	1
Mr. Robert W. Jones Advanced Projects Manager Hughes Aircraft Company Mail Station D 132 Culver City, California 90230	1
Dr. C. Giori IIT Research Institute 10 West 35 Street Chicago, Illinois 60616	
Dr. R. S. Roe Department of Materials Science and Metallurgical Engineering University of Cincinnatti Cincinnati, Ohio 45221	1
Dr. Robert E. Cohen Chemical Engineering Department Massachusetts Institute of Technology Cambridge, Massachusetts 02139	1
Dr. T. P. Conlon, Jr., Code 3622 Sandia Laboratories Sandia Corporation Albuquerque, New Mexico	1

TECHNICAL REPORT DISTRIBUTION LIST, 356A

	No. Copies
Dr. Martin Kaufman Code 38506 Naval Weapons Center China Lake, California 93555	1
Professor S. Senturia Department of Electrical Engineering Massachusetts Institute of Technology Cambridge, Massachusetts 02139	1
Dr. T. J. Reinhart, Jr., Chief Composite and Fibrous Materials Branch Nonmetallic Materials Division Department of the Air Force Air Force Materials Laboratory (AFSC) Wright-Patterson AFB, Ohio 45433	1
Dr. J. Lando Department of Macromolecular Science Case Western Reserve University Cleveland, Ohio 44106	1
Dr. J. White Chemical and Metallurgical Engineering University of Tennessee Knoxville, Tennessee 37916	1
Dr. J. A. Manson Materials Research Center Lehigh University Bethlehem, Pennsylvania 18015	1
Dr. R. F. Helmreich Contract RD&E Dow Chemical Co. Midland, Michigan 48640	1
Dr. R. S. Porter Department of Polymer Science and Engineering University of Massachusetts Amherst, Massachusetts 01002	1
Professor Garth Wilkes Department of Chemical Engineering Virginia Polytechnic Institute and State University Blacksburg, Virginia 24061	1
Professor C. S. Paik Sung Department of Materials Sciences and Engineering Room 8-109 Massachusetts Institute of Technology Cambridge, Massachusetts 02139	1
Professor Brian Newman Department of Mechanics and Materials Science Rutgers, The State University Piscataway, New Jersey 08854	1
Dr. John Lundberg School of Textile Engineering Georgia Institute of Technology Atlanta, Georgia 30332	1